

Paper presented at the 58th Electric Furnace Conference
Orlando, USA, 13.-14.11.2000
Proceedings p. 893 - 904

Observation and control of AOD process with exhaust gas measurement

Franz-Josef Wahlers
Karl-Heinz Schubert
Christian Burkat

Krupp Thyssen Nirosta
Alleestrasse 165
D - 44793 Bochum
Germany
Fax +49 234 919-5435

Siegfried Köhle
Christoph Bendel

Betriebsforschungsinstitut (BFI)
Sohnstrasse 65
D - 40237 Düsseldorf
Germany
Fax +49 211 6707-310

Key Words: AOD converter, stainless steel, decarburisation, exhaust gas, process observation, blowing control

INTRODUCTION

For the production of stainless steels in the Bochum steel plant of Krupp Thyssen Nirosta, scrap and alloys are molten in an AC electric arc furnace of 150 t tap weight. Feed metal from the furnace is decarburised and desulphurised in two 75 t top lance AOD converters ¹.

Within the AOD process control system, which is shortly described below, one converter has been equipped with exhaust gas measurement devices. The paper deals with metallurgical process observation by means of carbon and oxygen balances and describes some features to improve the dynamic control of the AOD process.

PROCESS CONTROL SYSTEM

The process control system for refining of high-chromium steels in the AOD converter comprises process observation as well as control of blowing, addition of alloys, additives and reduction materials ². The structure of the control system with its essential functions is shown in **Fig. 1**. The process observation uses measured values of

- oxygen and argon/nitrogen input rates
- flow rate and composition of the exhaust gas

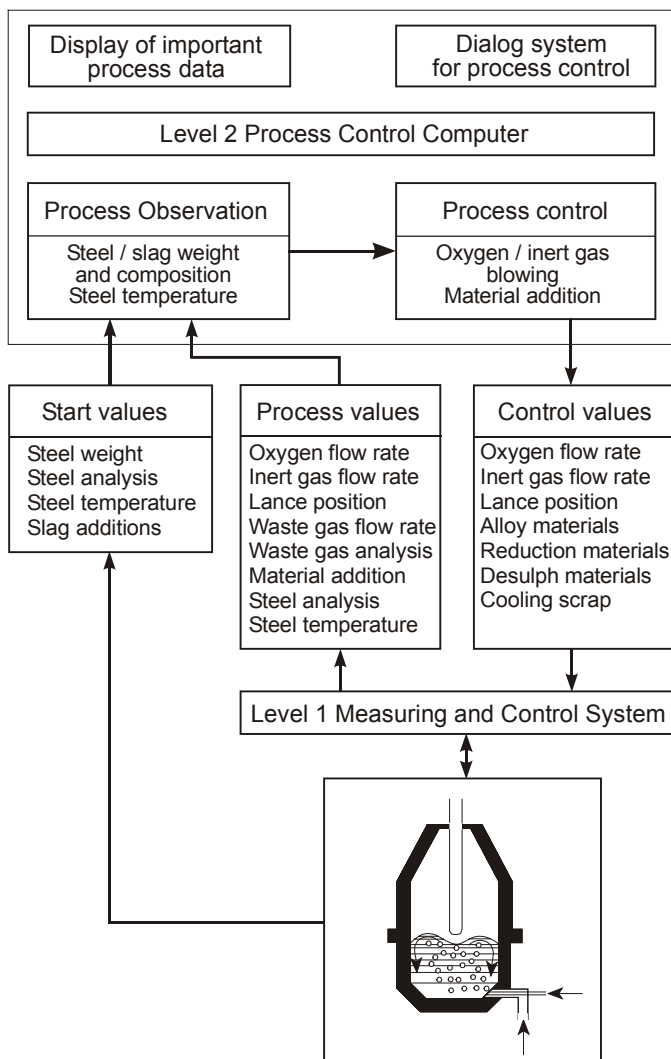


Fig. 1: Structure of the AOD process control system

METALLURGICAL PROCESS OBSERVATION

The metallurgical process observation calculates the weight and the composition of steel and slag as shown by its block diagram in **Fig. 2**. The calculation starts from corresponding initial values at the beginning of blowing. The carbon and oxygen balances are mainly based on the exhaust gas flow rate and composition. The results of the cyclically running balance calculations are updated after several events. In the case of material addition, its influence on weight and composition of the melt is taken into account. When an analysis is transferred from the laboratory computer, the calculated steel composition is adapted to the analysed one, taking into account the inputs and losses of the different elements which occurred after the sample had been taken.

Exhaust Gas Measurement

The exhaust gas system of the AOD converter is schematically shown in **Fig. 3** together with measured variables. The sample for analysing the exhaust gas composition is taken from the clean gas in the stack. The CO and CO₂ concentrations are measured on the basis of infrared absorption, the O₂ concentration measurement uses

- material additions from the bins
- steel temperature measured with the sub lance
- steel analysis from the laboratory computer which are transmitted from the level 1 measuring and control system.

The actual process state is calculated from these values by means of carbon, oxygen and energy balances, starting from the initial state of the heat at beginning of blowing. The process state is defined by steel and slag weight and composition as well as steel temperature.

The rates of decarburisation and chromium oxidation as well as carbon content and steel temperature are displayed on a graphic screen at the control panel, providing useful information about the process behaviour. Other screens display flow rates and consumption of all process gases and serve for the dialog between converter operator and computer.

On basis of the observed process state, setpoint values for the flow rates of oxygen and inert gas through lance and tuyeres are calculated. Alloys for adjustment of the aim analysis are calculated at minimal cost together with additives for reduction and desulphurisation. Addition of cooling scrap is calculated in order to meet the final aim temperature of the heat. All setpoint values are transmitted to the level 1 control system.

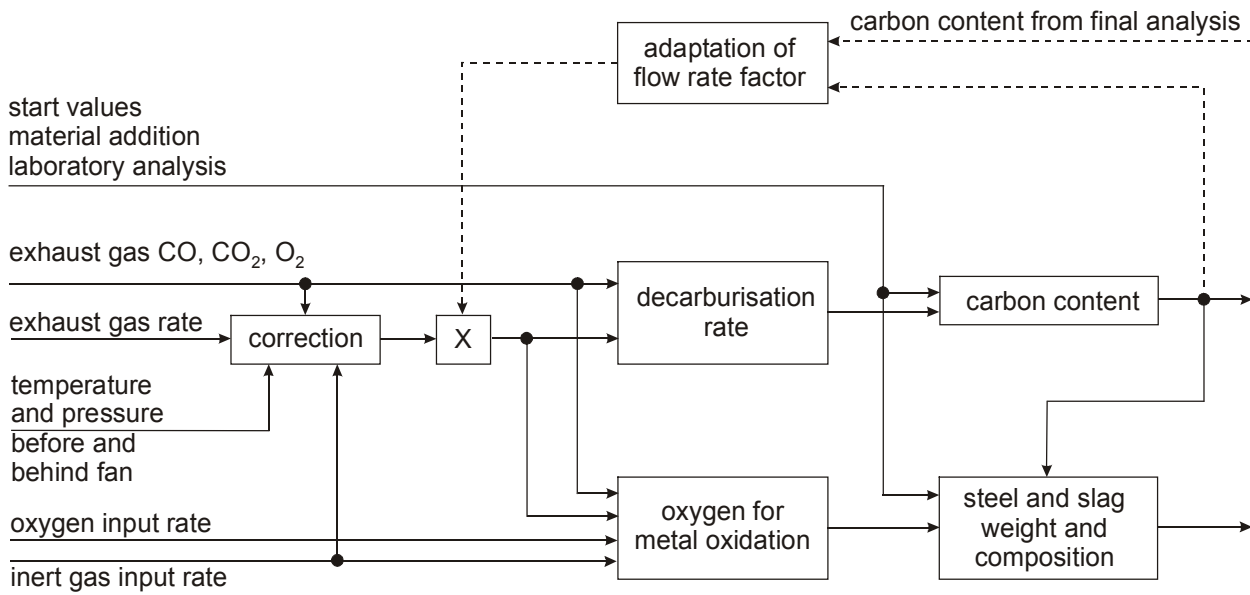


Fig. 2: Block diagram of metallurgical process observation

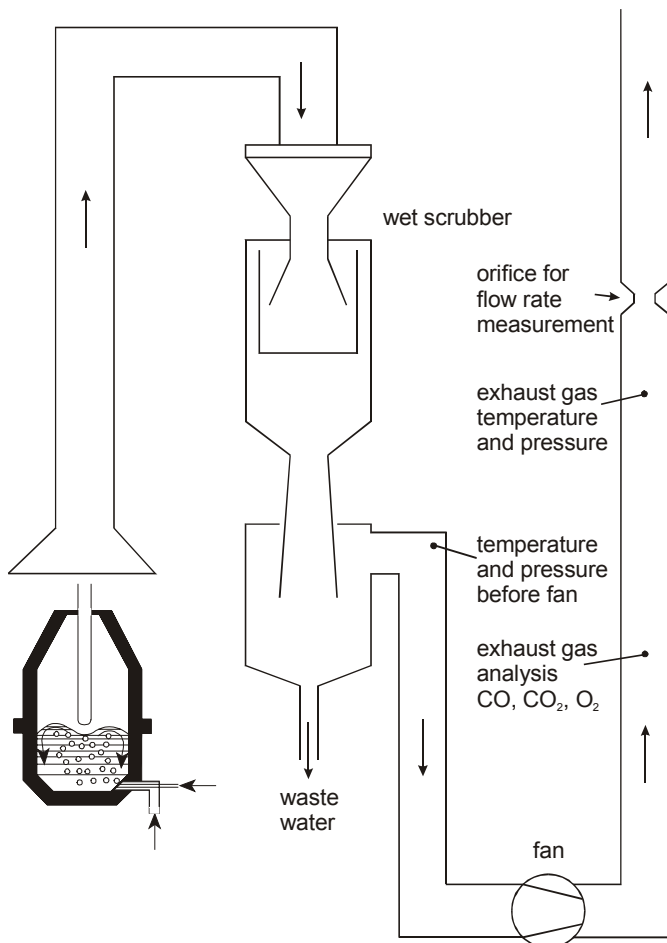


Fig. 3: Exhaust gas system with measurement

the effect of paramagnetism. The measured concentration values are subject to a time delay of about 25 seconds because of the transport and preparation of the gas sample and the response time of the analysing equipment. For this reason the other instantaneously measured values are delayed by a corresponding time before being combined with the exhaust gas concentrations.

The exhaust gas flow rate is measured with a differential-pressure device installed in the stack. The flow rate value from the measuring transmitter is corrected for standard conditions of dry gas, taking into account the actual values of pressure, temperature, density and humidity of the exhaust gas:

- The temperature and the pressure are measured.
- The exhaust gas density is calculated according to its composition. The concentrations of CO, CO₂ and O₂ are analysed, the Ar concentration is determined from the argon input rate, and the remainder is assumed to be nitrogen.
- The exhaust gas humidity is calculated from pressure and temperature values measured before and behind the fan, assuming that before the fan the gas is saturated with water vapour from the wet scrubbers.

Carbon Balance

The carbon balance calculates the decarburisation rate and the remaining carbon content in steel. With the variables

K_{CO} exhaust gas CO concentration,

K_{CO_2} exhaust gas CO₂ concentration,

Q_G exhaust gas flow rate,

W_M steel weight,

W_{M0} initial steel weight,

C_0 initial carbon content,

W_{CZ} weight of carbon from material additions,

the decarburisation rate is

$$-\frac{dC}{dt} = \frac{12 \text{ kg}}{22.4 \text{ m}^3} \cdot (K_{CO} + K_{CO_2}) \cdot Q_G \cdot \frac{100\%}{W_M} , \quad (1)$$

the weight of removed carbon is

$$W_{CV} = \frac{12 \text{ kg}}{22.4 \text{ m}^3} \cdot \int (K_{CO} + K_{CO_2}) \cdot Q_G \cdot dt , \quad (2)$$

and the balanced carbon content is

$$C = \left(\frac{C_0}{100\%} \cdot W_{M0} + W_{CZ} - W_{CV} \right) \cdot \frac{100\%}{W_M} . \quad (3)$$

As indicated in Fig. 2, the exhaust gas flow rate is multiplied by an additional correction factor. This factor is adapted by a smoothing algorithm after every heat, when the balanced carbon removal can be compared to that one which is calculated from the carbon contents analysed before and after decarburisation, and from carbon input by material additions. With this adaptation, slowly varying errors of the carbon balance are compensated, so that the error mean value is always kept close to zero.

Oxygen Balance

The oxygen balance calculates the part of the blown oxygen which leads to an oxidation of metallic elements or, on a minor scale, is absorbed by the melt. If it is assumed that no CO from decarburisation is post-combusted in the converter with oxygen from the lance, the rate of oxygen for metal oxidation

$$Q_{O2M} = Q_{O2B} - 0.5 \cdot (K_{CO} + K_{CO_2}) \cdot Q_G \quad (4a)$$

can be calculated by a simple oxygen balance. Taking into account the possibility of CO post-combustion in the converter, the oxygen balance is extended to

$$Q_{O2M} = Q_{O2B} + 0.21 \cdot Q_F - (0.5 \cdot K_{CO} + K_{CO_2} + K_{O_2}) \cdot Q_G , \quad (4b)$$

now also including the input of oxygen from entrained air with 21% of oxygen, and the output of pure oxygen in the exhaust gas. With this extended oxygen balance, also the degree of CO post-combustion by oxygen from the lance and a lance efficiency factor can be determined.

The flow rate of entrained air is calculated by an inert gas balance, assuming that the exhaust gas contains besides its analysed components only nitrogen and argon with 79% as sum of their concentrations in air:

$$Q_F = \frac{1}{0.79} \cdot [(1 - K_{CO} - K_{CO_2} - K_{O_2}) \cdot Q_G - Q_{N_2B} - Q_{ArB}] \quad (5)$$

The necessary variables for these calculations are:

- Q_{O_2B} oxygen input rate,
- Q_{N_2B} nitrogen input rate,
- Q_{ArB} argon input rate,
- K_{CO} exhaust gas CO concentration,
- K_{CO_2} exhaust gas CO₂ concentration,
- K_{O_2} exhaust gas O₂ concentration,
- Q_G exhaust gas flow rate.

The calculated total oxygen for metal oxidation is partitioned to oxidation of aluminium and silicon at first, and to subsequent oxidation of chromium and other metallic elements with statistically determined percentages of the remaining oxygen. When silicon material is added after blowing, this calculation takes into account the reduction of chromium oxide from the slag by the oxidation of silicon. Together with the carbon balance, the oxygen balance thus calculates the changing weights and compositions of steel and slag by decarburisation and metal oxidation, taking also into account all material additions and the analysis of intermediate steel samples.

Example Heat

Measured and calculated values are given in **Fig. 4** for an example heat. The upper diagram contains the flow rates of oxygen and inert gas through the tuyeres and the lance. The concentrations of CO, CO₂ and O₂ in the exhaust gas are plotted in the middle. Because of intensive CO post-combustion by oxygen from the entrained air, the CO concentration remains below 0.2%.

The lower diagram presents the decarburisation rate calculated by equation (1) and the balanced carbon content from equation (3). It can be seen that the decarburisation rate decreases towards the end of the first blowing step with high oxygen and low inert gas flow rates. When for the second blowing step the

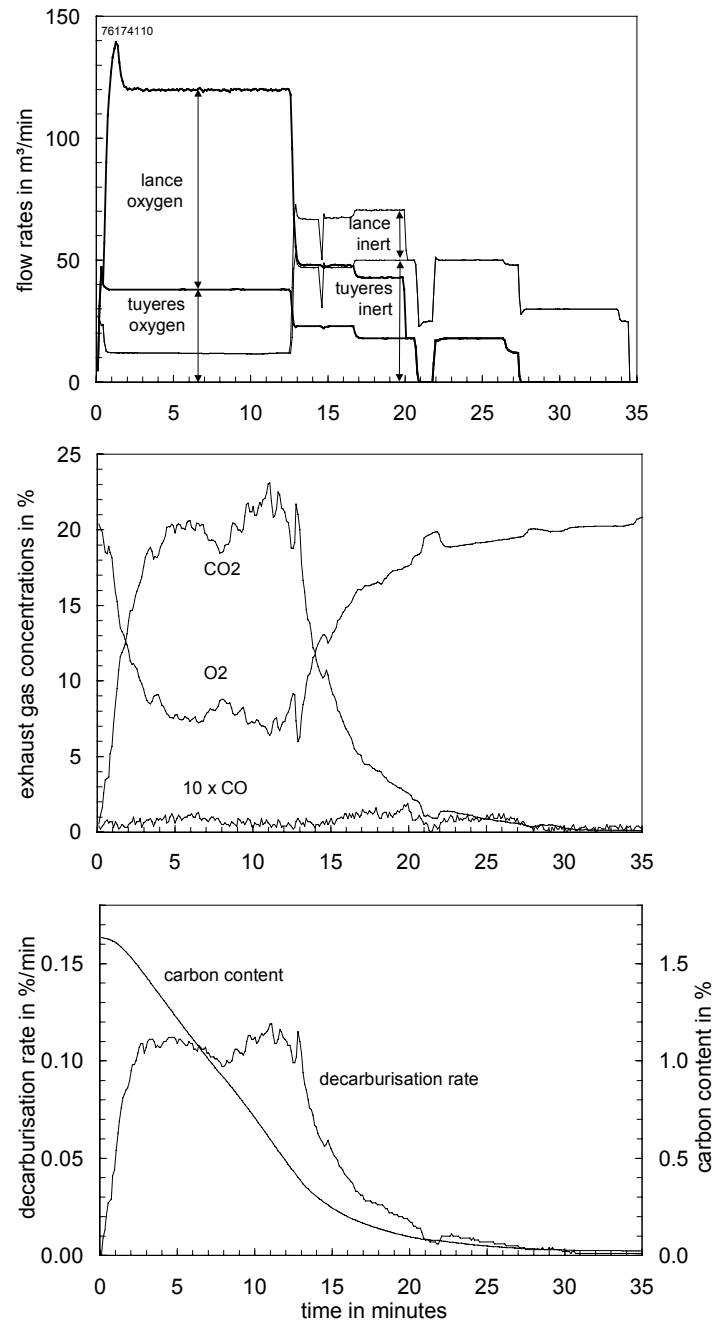


Fig. 4: Measured and calculated values of a heat

oxygen rates are lowered and the inert gas rates are raised, the decarburisation rate increases by a short peak before it decreases nearly exponentially.

In **Fig. 5** the decarburisation rate is plotted versus the carbon content for the same heat as before. This plot, called “phase diagram” in the theory of dynamic systems, presents the dependence of the decarburisation rate on the carbon content more clearly than their plots versus time in the preceding figure. This dependence will be discussed below in more detail.

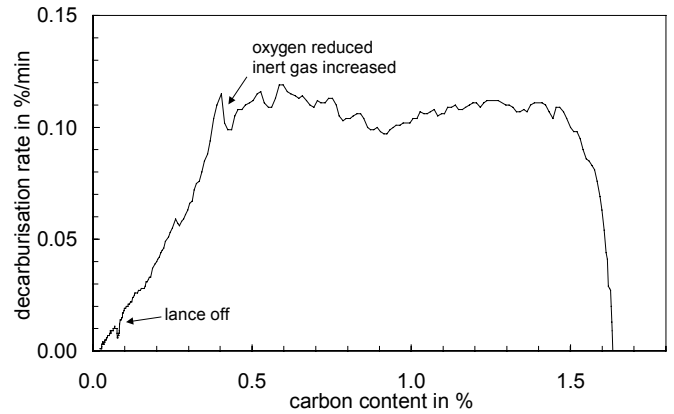


Fig. 5: Decarburisation rate versus carbon content

Process Observation Monitor

The decarburisation versus carbon diagram can be displayed on the process observation monitor at the control panel of the AOD converter, as shown in the upper left part of **Fig. 6**. Alternatively the time courses of decarburisation and chromium oxidation rates can be displayed. Calculated steel carbon content and temperature are shown in the upper right diagram. In the lower part, several measured and calculated values are presented.

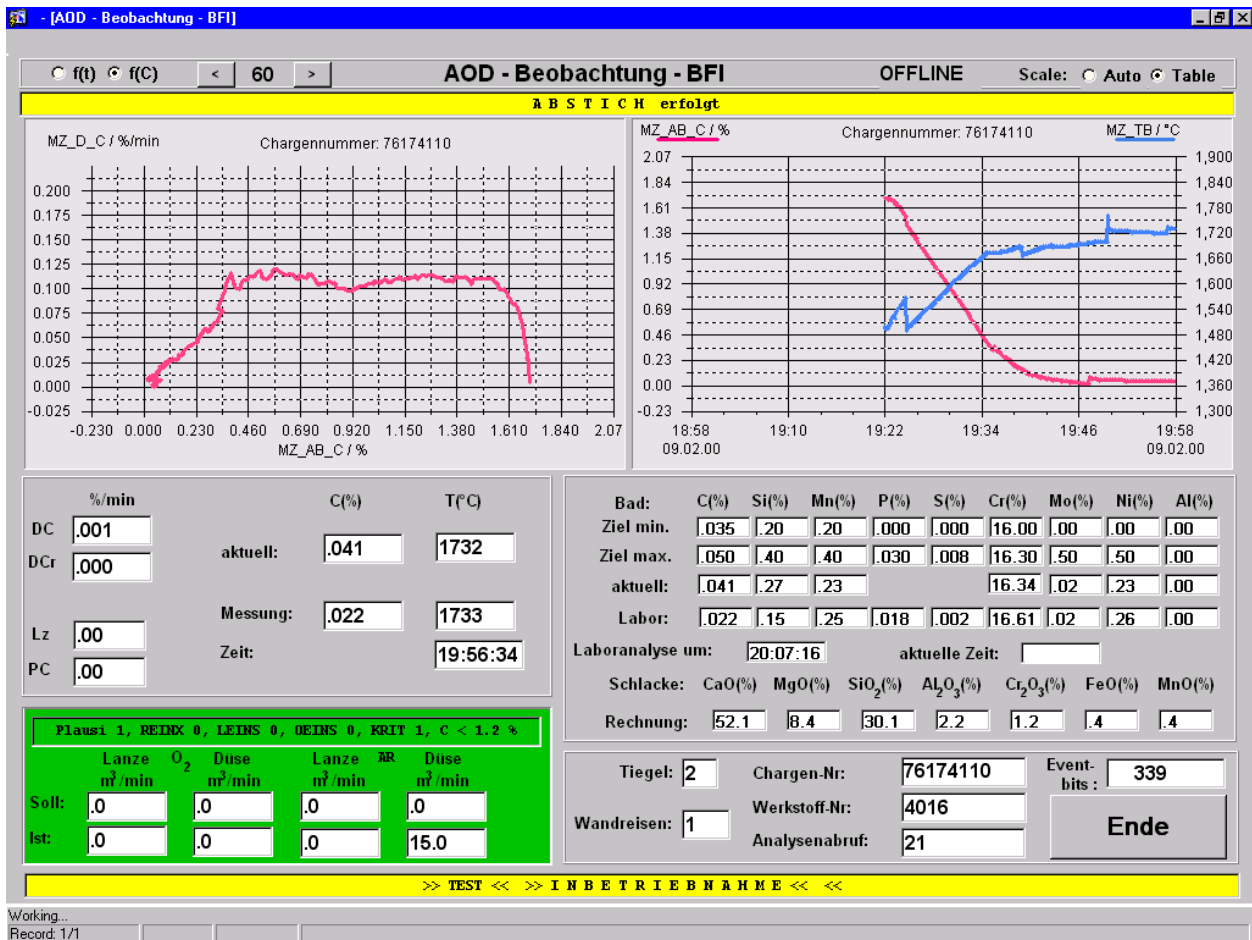


Fig. 6: Observation monitor for the AOD process

Statistical Evaluation

The accuracy of the carbon and oxygen balance calculation is determined after every heat, when the final steel analysis is available for comparison. As an example, results from statistical evaluation of about 200 heats are presented below.

Carbon balance – The balanced carbon removal from equation (2) is plotted in **Fig. 7** versus that value which is calculated with the carbon content from the final analysis:

$$W_{CT} = \frac{C_0}{100\%} \cdot W_{M0} + W_{CZ} - \frac{C_T}{100\%} \cdot W_{MT} , \quad (6)$$

- C_0 initial carbon content,
- W_{M0} initial steel weight,
- W_{CZ} weight of carbon from material additions,
- C_T analysed carbon content after AOD,
- W_{MT} steel weight after AOD.

The linear regression between both values has a rather high coefficient R^2 of determination. The carbon balance error, i. e. the difference between both values, is zero on average, thanks to the adaptation of the exhaust gas flow rate factor after every heat. The error standard deviation of ~5% is not high with respect to the numerous input values of the carbon balance, i. e. initial steel weight and carbon content, weight of carbon from material additions, flow rate and composition of the exhaust gas. But after decarburisation of e. g. 1.6% C, for the balanced carbon content this results in an error standard deviation of 0.08% C which is higher than the low final carbon content itself. It will be discussed below how the accuracy of the calculated carbon content can be improved by a model based correction of the carbon balance.

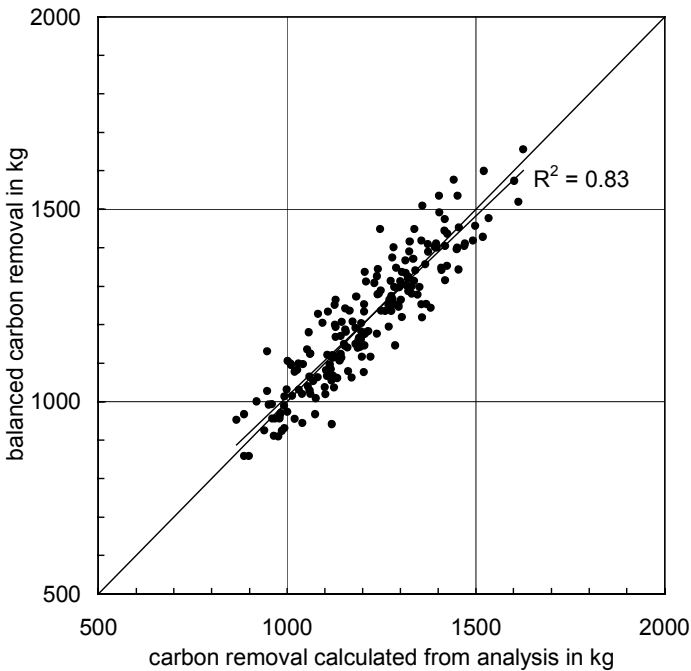


Fig. 7: Comparison of carbon removal

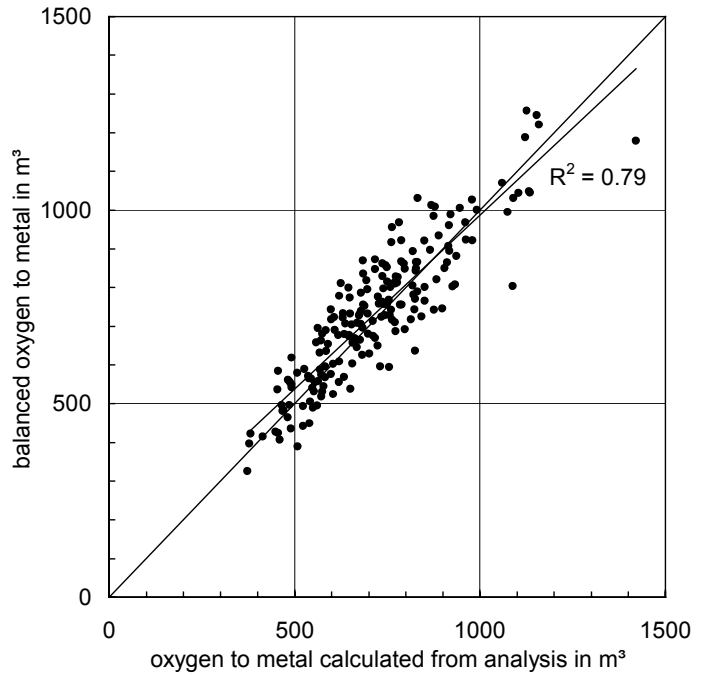


Fig. 8: Comparison of oxygen for metal oxidation

Oxygen balance – In **Fig. 8** the balanced volume of oxygen for metal oxidation, i. e. the integrated rate from equation (4), is plotted versus that value which is calculated with the final analysis:

$$V_{O_{2MT}} = \sum_Y F_{OY} \cdot \left(\frac{Y_0}{100\%} \cdot W_{M0} + W_{YZ} - \frac{Y_T}{100\%} \cdot W_{MT} \right), \quad Y = \text{Al, Si, Mn, Cr}, \quad (7)$$

F_{OY} stoichiometric oxygen for oxidation of element Y,

Y_0 initial content of element Y,

W_{M0} initial steel weight,

W_{YZ} weight of element Y from material additions,

Y_T analysed content of element Y after AOD,

W_{MT} steel weight after AOD.

The coefficient R^2 of determination is nearly as high as for the carbon balance, the error mean value is approximately zero, and the error standard deviation is about 10%. This oxygen error corresponds to an error standard deviation of 0.13% Si for the content of silicon after reduction.

By evaluating this error it has to be considered that the oxygen balance does not include some oxygen input from oxides in the carry-over slag of the electric arc furnace, because individual weight and composition of this slag are not known. These oxides - together with those generated during blowing - are reduced afterwards by oxidation of added silicon, so that they contribute to the oxygen calculated by equation (7). On the other side this equation does not include some oxygen which may have been used for oxidation of iron, so that both missing items partially compensate each other.

IMPROVEMENT OF PROCESS OBSERVATION AND CONTROL

For improving observation and control of the AOD process, a simple model helps to understand the principal process characteristics. Vice versa, such a model can be verified by means of the observed process behaviour.

Decarburisation Model

As can be seen from Fig. 4 and 5, the main decarburisation period is characterised by an approximately constant decarburisation rate which is mainly determined by the oxygen input rate. In the final period of decarburisation however, its decreasing rate depends on the distance of the carbon content from its equilibrium³:

$$D_C = - \frac{dC}{dt} = \frac{1}{T_C} \cdot (C - C_Q), \quad (8)$$

C carbon content,

C_Q equilibrium carbon content,

T_C time constant of decarburisation.

From the equilibrium relations for oxidation of chromium and carbon results the equilibrium carbon content⁴:

$$C_Q = \frac{(C_{Cr} \cdot f_{Cr})^{2/3}}{f_C} \cdot \frac{K_{Cr}^{1/3}}{K_C} \cdot \frac{1}{a_{ox}^{1/3}} \cdot P_{CO}, \quad (9a)$$

- Cr_Q equilibrium chromium content,
 f_{Cr} chromium activity coefficient,
 f_C carbon activity coefficient,
 K_{Cr} chromium equilibrium coefficient,
 K_C carbon equilibrium coefficient,
 a_{ox} activity of chromium oxide Cr_2O_3 ,
 P_{CO} partial pressure of CO.

In the abbreviation of above equation

$$C_Q = F_{CO}(Cr, Ni, T, a_{ox}) \cdot P_{CO} , \quad (9b)$$

the factor F_{CO} depends on

- contents of Cr, Ni and other elements which affect the activities of Cr and C,
- steel temperature which has a strong effect on the chromium equilibrium,
- activity of chromium oxide which depends on oxidised chromium.

With the conversion factor

$$F_{DC} = \frac{22.4 \text{ m}^3}{12 \text{ kg}} \cdot \frac{W_M}{100\%} \quad (10)$$

between the decarburisation rate D_C of a melt with steel weight W_M and the flow rate of generated CO, its partial pressure

$$P_{CO} = \frac{F_{DC} \cdot D_C}{F_{DC} \cdot D_C + Q_P} \cdot P_A \quad (11)$$

depends on its dilution by the inert gas with flow rate Q_P . For decarburisation by oxygen from the lance, the total gas pressure is given by the atmospheric pressure P_A under which AOD converters are operated. For decarburisation by oxygen from the tuyeres, the CO partial pressure in the ascending gas bubbles approximately equals that one near below the bath surface, as a result of the decreasing ferrostatic pressure and the increasing CO generation⁵. Therefore equation (11) may be applied for the total decarburisation.

Carbon Balance Correction

When equation (8) is solved for the carbon content, with equations (9) and (11) results its non-linear relation

$$C = T_C \cdot D_C + \frac{D_C}{D_C + Q_P / F_{DC}} \cdot F_{CO} \cdot P_A \quad (12)$$

to the decarburisation rate, which is in accordance with the dependence between both variables during the final decarburisation period shown in Fig. 5. This non-linear dependence, tending more and more towards the origin with decreasing decarburisation rate, is typical for the AOD process. It results from the dilution of CO by the inert gas with high flow rate, described by the fraction in equation (12).

The presented model is also valid for decarburisation of high chromium steels in the VOD process, but with a low pressure instead of the atmospheric pressure. Because of the much lower inert gas flow rate for VOD, CO dilution has an effect only at lowest decarburisation rates. Therefore, during most of the final decarburisation

period, the relation between the decarburisation rate and the carbon content is strongly linear, tending to about 0.015% C for vanishing decarburisation. Based on this, the balanced carbon content can be corrected by a dynamically performed linear regression analysis between both variables. Applying this method at a VOD plant, the error standard deviation of the corrected carbon content at the end of decarburisation was reduced to 0.005% C, i. e. by a factor of 3 compared to the balanced carbon content⁴.

Despite of the non-linear relation between the decarburisation rate and the carbon content for AOD, the same method to correct the balanced carbon content by linear regression was applied in a first step. The frequency distribution of the resulting carbon error, i. e. the difference between the carbon content calculated at treatment end and the subsequently analysed carbon content, is shown in Fig. 9 for about 100 heats. The error standard deviation is reduced to ~0.02% C, i. e. by a factor of 4 in comparison to the value given above from statistical evaluation of the carbon balance. It is intended to improve the carbon balance correction by taking into account the AOD specific non-linear relation.

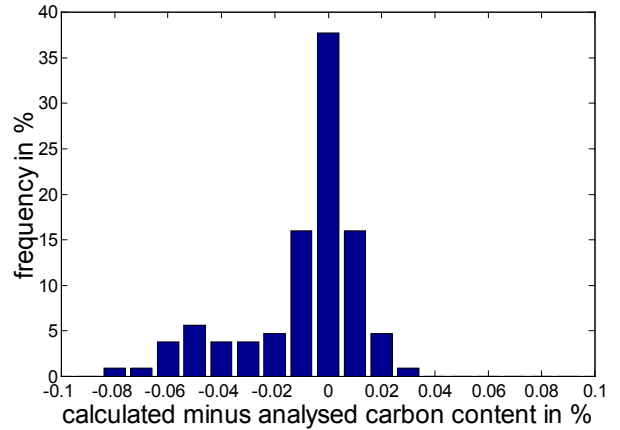


Fig. 9: Error after carbon balance correction

Dynamic Blowing Control

In Fig. 10 it is indicated which parts of the total oxygen input from Fig. 4 are used for decarburisation and for metal oxidation. When decarburisation starts to decrease a few minutes before the end of the first blowing step, the model described above becomes valid, i. e. according to equation (8) decarburisation is now limited by the decreasing distance between the carbon content and its equilibrium. When oxygen input is reduced then, the carbon equilibrium is lowered by the increased inert gas rate, see Fig. 4, so that decarburisation is enforced and consumes some of the oxygen dissolved in steel. With the steadily decreasing distance from the equilibrium, decarburisation is lowered more and more, and the excess of oxygen input results in metal oxidation.

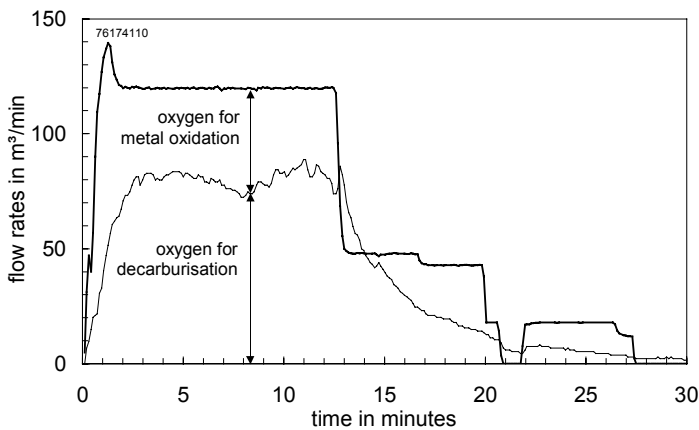


Fig. 10: Oxygen for decarburisation and for metal oxidation

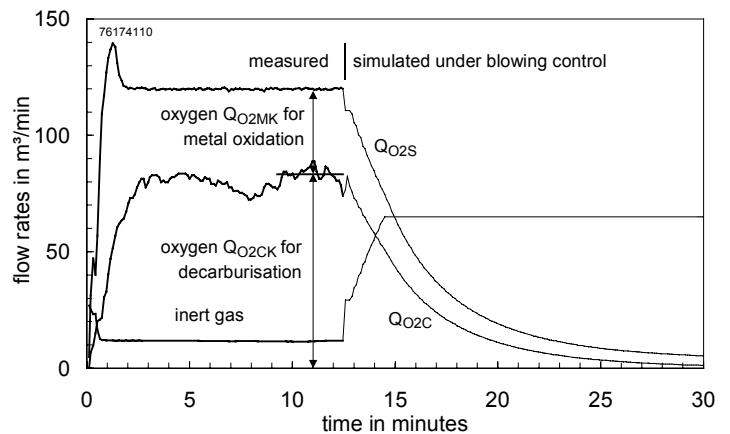


Fig. 11: Scheme of dynamic blowing control

This example demonstrates that the oxygen input rate should be reduced continuously during final decarburisation, according to its decreasing oxygen demand, in order to keep metal oxidation as low as possible. A certain excess of oxygen for metal oxidation has however to be offered, because otherwise decarburisation would be more restricted by a shortage of oxygen than by thermodynamic process conditions.

The oxygen control strategy is schematically shown in **Fig. 11**. When decarburisation decreases at the end of its approximately constant period, dynamic oxygen control is started. The continuously decreasing oxygen demand for decarburisation is known from process observation. The excess oxygen for metal oxidation is deduced from the situation observed before start of the final decarburisation period and may be controlled between two extremes. The upper limit is that the preceding amount of oxygen for metal oxidation is further provided. For the lower limit this oxygen is reduced by the same ratio which is observed for decarburisation oxygen. The setpoint for the total oxygen input rate is placed between both extremes with only one control parameter:

$$Q_{O2S} = Q_{O2C} \cdot \left[1 + (1 - F_S) \cdot \frac{Q_{O2MK}}{Q_{O2CK}} \right] + F_S \cdot Q_{O2MK} , \quad (13)$$

- Q_{O2MK} oxygen for metal oxidation before final decarburisation,
- Q_{O2CK} oxygen for decarburisation before final decarburisation,
- Q_{O2C} oxygen for decarburisation during final decarburisation,
- F_S parameter for oxygen input control.

In Fig. 11 the oxygen input rate was calculated with $F_S = 0.1$. With the reduction of oxygen, the inert gas input is increased in order to lower the carbon equilibrium by CO dilution and to keep the decarburisation rate as high as possible. Inert gas input is restricted to limits given by plant or process technology or by economical consideration. The total oxygen and inert gas input is divided between lance and tuyeres by the same ratio as during the period of constant decarburisation. When the gas flow rate for the lance becomes too small, its operation is finished.

SUMMARY

An AOD converter for stainless steel production at the Bochum steel plant of Krupp Thyssen Nirosta has been equipped with measurement devices for the exhaust gas flow rate and CO, CO₂, O₂ concentrations. By means of carbon and oxygen balances, the rates of decarburisation and metal oxidation as well as weight and composition of steel and slag are continuously calculated.

The accuracy of the balanced carbon content can be improved by using the characteristic dependence of the decarburisation rate on the carbon content during the final decarburisation period. With dynamic blowing control according to the decreasing oxygen demand for decarburisation during this period, metal oxidation can be minimised and the decarburisation rate can be kept as high as possible under given thermodynamic restrictions.

ACKNOWLEDGMENTS

This paper includes results from work carried out with a financial grant from the European Coal and Steel Community.

REFERENCES

1. F.-J. Wahlers, M. Walter and H. Zörcher, Production of stainless steels at Krupp Thyssen Nirosta (in German), Stahl u. Eisen, Vol. 118, 1998, No. 9, pp. 95-98
2. J. Reichel, S. Köhle, K.-H. Schubert, F.-J. Wahlers and H. Zörcher, Observation and control of the refining of high-chrome steels by the KCB-S process (in German), Stahl u. Eisen, Vol. 113, 1993, No. 9, pp. 83-89
3. S. Asai and K. Szekely, Decarburization of Stainless Steel, Metallurgical Transactions, Vol. 5, 1974, No. 3, pp. 651-657 and No. 7, pp. 1573-1580
4. S. Köhle, J. Reichel, K.-H. Heinen and D. Dittert, Dynamic Modelling and Control of the VOD-Process, 5th International Iron and Steel Congress, Washington DC 1986, Process Technology Proc., pp. 257-265
5. T. Deb Roy and D. G. C. Robertson, Mathematical model for stainless steelmaking, Ironmaking and Steelmaking, 1978, No. 5, pp. 198-210